

## Mapping dominant tree species over large forested areas using Landsat best-available-pixel image composites

Shanley D. Thompson<sup>a\*</sup>, Trisalyn A. Nelson<sup>a</sup>, Joanne C. White<sup>b</sup>, Michael A. Wulder<sup>b</sup>

<sup>a</sup> Spatial Pattern Analysis and Research Lab, Department of Geography, University of Victoria, PO BOX 3060, Victoria, British Columbia, Canada, V8W 3R4

<sup>b</sup> Canadian Forest Service (Pacific Forestry Centre), Natural Resources Canada, 506 Burnside Road West, Victoria, British Columbia, Canada, V8Z 1M5

\* Corresponding author e-mail: [sdthomps@uvic.ca](mailto:sdthomps@uvic.ca)

### Pre-print of published version

#### Reference:

Thompson, S.D., Nelson, T.A., White, J.C., Wulder, M.A. 2015. Large area mapping of tree species using composited Landsat imagery. *Canadian Journal of Remote Sensing* 41(3): 203-218.

#### DOI:

10.1080/07038992.2015.1065708

#### Disclaimer:

The PDF document is a copy of the final version of this manuscript that was subsequently accepted by the journal for publication. The paper has been through peer review, but it has not been subject to any additional copy-editing or journal specific formatting (so will look different from the final version of record, which may be accessed following the DOI above depending on your access situation).

## **Mapping dominant tree species over large forested areas using Landsat best-available-pixel image composites**

**Abstract:** Remotely sensed image composites that are pixel-, rather than, scene-based, are increasingly feasible over large areas and fine spatial resolutions. For large jurisdictions that utilize remotely sensed imagery for ecosystem mapping and monitoring, pixel-based composites enable a wider range of applications, at higher quality. The goal of this study was to model spatial distributions of six tree species over a large forested area of Saskatchewan, Canada (>39 million ha) at 30 m spatial resolution using a multi-year Best-Available-Pixel (BAP) Landsat composite. We tested the influence of the BAP composite on the resultant maps by comparing species composition and configuration for areas where imagery was from a single sensor, year, and day of year, to areas with variable composite characteristics. Model error rates ranged from 0.09% to 0.24%, Area-Under-the-Curve values approaching 1, and met ecological expectations. The BAP composite was found to have little effect on model outcomes, with composition and configuration values in non-reference areas being similar for all species but one, which had an unexpected configuration. Moreover, sensor, year, and day of year were similar for reference and non-reference blocks for all species. Results indicate Landsat BAP image composites are useful for generating large-area maps of tree species distributions.

**Keywords:** forest, vegetation, modelling, composite, Canada, species, spatial

**Abbreviations:** Best-Available Pixel (BAP), National Forest Inventory (NFI), Normalized Burn Ratio (NBR), Area Under the Curve (AUC), Receiver Operating Characteristic (ROC)

### **INTRODUCTION**

Effective forest management requires knowledge of the spatial distribution of tree species composition and abundance. Species information is used to assess risks and impacts associated with a variety of natural or anthropogenic disturbances, including fires, insect and invasive plant infestations, and resource extraction. Species composition and abundance, together with other metrics such as species richness, species endemism, and rarity are also important metrics of biodiversity that can be used to guide conservation planning (Fleishman et al., 2006) and ecosystem service assessment (Kremen, 2005). In addition, climate change may alter the distribution of tree species in the future (Coops and Waring, 2010; Hamann and Wang, 2006; Pfeifer-Meister et al., 2013; Thuiller et al., 2005), and knowledge of the current distribution is the first step in attempting to understand, monitor, and as possible, manage those changes.

Despite the importance and various needs for tree species distribution data, the availability of these data is limited. Some projects may benefit from the tree observations and vegetation plot data compiled and shared via online databases such as the Global Biodiversity Information Facility (gbif.org) and the Global Index of Vegetation-Plot Databases (givd.info). However, these data remain spatially incomplete and biased towards easily accessible or protected areas (García Márquez et al., 2012; Hortal et al., 2007). Expert range maps (e.g., Little 1971) provide a general indication of where species occur, but overestimate the true distribution of a species (Jetz et al., 2007; McPherson and Jetz, 2007). Strategic-level forest inventories are typically undertaken in areas that have the capacity to support commercial timber production. Outside these areas, forest inventory data may be available, generally with less spatial and attributional detail, according to the forest monitoring needs in the area. In Canada, for example,

forest inventories are common in the more intensively managed southern forests (Falkowski et al., 2009), while only the sample-based National Forest Inventory aims to systematically characterize forest resources outside of managed forest areas (Gillis et al., 2005; Wulder et al., 2004b).

The paucity of detailed inventory data makes satellite remote sensing a necessary source of information from which species distributions can be mapped or modelled over large areas. High spatial resolution imagery can offer opportunities for mapping individual tree structure and composition (Wulder et al., 2004a), but the spatial image extents are limited (e.g., 10 by 10 km) requiring many images (with variable view angles and illumination conditions) to map a given area, leading to high cost. Imagery with larger extents are often of interest for mapping larger areas; however, these data come with pixel sizes that subsume many individual objects and landscape features, diminishing the variance between pixels, and limiting the capacity to map high levels of categorical detail, such as tree species composition. Issues such as atmospheric contamination (i.e., clouds, haze) further limit scene availability and confound mapping efforts. Several recent advances address some of these shortcomings and offer increased capacity to use remotely sensed data for predictive species mapping over large areas at higher spatial resolutions. Specifically, as of 2008, satellite imagery from the Landsat series of sensors, extending from 1972 to present, are freely available to the public (Woodcock et al., 2008; Wulder et al., 2012). Free and open access to analysis-ready Landsat data has enabled considerable innovative capacity (Wulder and Coops, 2014). Combined with improved computing power that facilitates large-area image compositing approaches (Roy et al., 2010) as well as the applications-focused best-available-pixel (BAP) approaches of Griffiths et al. (2013) and White et al. (2014), spatially exhaustive coverage of large areas at a spatial resolution of 30 m in a systematic and transparent fashion is now possible. For instance, compositing approaches can be based upon use of the best available observation for each pixel, with "best" being defined according to a set of scores for characteristics such as year, day of year (DOY), distance to cloud and cloud shadow, and sensor (Griffiths et al., 2013). Regional composites of medium spatial resolution imagery can be expected to become increasingly common (Griffiths et al., 2014). Detailed, efficient (large-area) maps of species distributions are a likely product of these compositing approaches, so long as the models are robust to some composite-imposed spectral variability. The goal of this research is to generate spatially detailed (30 m) distribution maps for six tree species over a large forested area of Canada using a multi-year Best-Available-Pixel (BAP) Landsat composite. A specific objective was to evaluate the impact of composite characteristics (i.e., DOY, year, and sensor) on model outcomes, which was assessed by the spatial pattern (composition and configuration) of the predictions.

## **METHODS**

### ***Study area***

The study area is approximately 39 million ha, and comprises the three forested ecozones of Saskatchewan, Canada. From North to South, these are the Taiga Shield, the Boreal Shield, and the Boreal Plains (Ecological Stratification Working Group, 1996) (Figure 1). The Boreal Plains is adjacent to the Prairie ecozone further south, and consists of rolling uplands and plains with a mixture of deciduous and coniferous vegetation species (McLaughlan et al., 2010). The Boreal Shield and Taiga Shield are characterized by a harsh climate and poorer soils, a greater proportion of coniferous tree species, and a lower diversity of plant species (McLaughlan et al.,

2010; Pastor et al., 1996). A variety of provincial forest inventory data exist in the managed forest area of the province (Figure 1), with varying spatial scales, levels of attribution, and temporal frequencies (Gillis et al., 2005; Saskatchewan Environment - Forest Service, 2004; Saskatchewan Ministry of Environment, 2009).

### ***Tree species distribution data***

Tree species distribution data were acquired from Canada's National Forest Inventory (NFI). The NFI consists of a grid of permanent sample plots distributed across the country, the majority of which are 2 km x 2 km "photo plots" (i.e., derived from air photo interpretations), within which multiple polygons are delineated indicating species composition and relative abundance. To reduce uncertainty at polygon edges, we removed 30 m (one pixel) from the inner edge of each polygon to ensure agreement between the inventory data and our predictor data (Verbyla and Hammond, 1995). To ensure adequate sample size and quality, we did not model species that occurred relatively infrequently or that occurred exclusively in polygons of heterogeneous composition ( $\leq 90\%$  of one species). In addition, polygons that were observed to have burned or been harvested since they were inventoried were removed, as were polygons that were very small in size (less than one pixel). Thus of the eleven tree species identified in the NFI photo plot data, we modelled the six most common (Table 1): black spruce (*Picea mariana*), trembling aspen (*Populus tremuloides*), jack pine (*Pinus banksiana*), white birch (*Betula papyrifera*), tamarack (*Larix laricina*), and white spruce (*Picea glauca*). Species that were present in insufficient numbers for modeling were *Abies balsamea*, *Acer negundo*, *Fraxinus pennsylvanica*, *Pinus contorta*, and *Populus balsamifera*. Our six target species may be found across all three forested ecozones in the province (McLaughlan et al., 2010).

### ***Image composite data***

We used a *multi-year* BAP surface reflectance composite as the source of spectral information in our distribution models. A detailed description of this and other compositing methods is provided in White et al. (2014). Briefly, candidate pixel observations were scored according to sensor (Landsat TM or ETM+), year, DOY, distance to clouds or cloud shadows, and haze, and the pixels with the highest score used to populate the final image composite. Our target was Landsat 5 TM imagery from August 1, 2010; however, candidate pixels included all observations acquired  $\pm 30$  days of August 1, 2009, 2010, and 2011, from Landsat 5 TM or 7 ETM+, as required to provide complete, cloud-free coverage of the study area. In Table 2 we show the number of unique images considered and selected for the final BAP composite for Saskatchewan as a whole (encompassing our study area as well as the Prairie Ecoregion). After scoring, 5% of pixel observations in the final composite of our study area were acquired from 2009 imagery, 69% from 2010 imagery, and 2% from 2011 imagery. The remaining 24% of pixels had BAP observations for both 2009 and 2011, and a proxy value was generated by taking the average of the 2009 and 2011 observations (see White et al., 2014). Pixels with proxy values were excluded from the analyses because there were no logical corresponding DOY or sensor values with which to assess relationships. In total, 95% of pixel observations were from Landsat 5 TM, and 5% from Landsat 7 ETM+. Almost 30% of pixel observations came within 7 days of the target DOY (August 1), with the remaining pixels acquired within 30 days of August 1. In the context of this study, which was designed to model tree species distributions, it is important to note that the majority of pixels (by area) in the composite came from imagery acquired in the 2010 target year and, furthermore that tree species distributions tend to change slowly over longer time horizons.

As such, the multi-year image composite used in this study is appropriate for modelling species distributions.

In order to reduce undesirable variability in the spectral reflectance values of the predictor variables used in our models (see Loveland & Merchant 1991), we calculated several spectral indices from the image composite data, and used these to exclude non-vegetated areas, and to the extent possible, non-forested areas from our analyses (Figure 2). Specifically, the Normalized Difference Vegetation Index (NDVI), and the Tasseled Cap (Crist and Cicone, 1984; Kauth and Thomas, 1976) Greenness (TCG), Brightness (TCB), and Wetness (TCW) indices were used to remove water, bare ground, urban areas, and sparsely vegetated areas. As well, the Normalized Burn Ratio (NBR) (Key and Benson, 2006), was used to identify and remove areas that had experienced fire in recent years, with the threshold NBR value chosen for this analysis (0.15) validated by data from the Canadian National Fire Database (Natural Resources Canada, 2010). An unsupervised classification of the Landsat spectral bands for the remaining pixels served to remove additional areas subsequently identified as cultivated land.

### ***Topographic data***

Topographic data were acquired from the freely available Canadian Digital Elevation Data (<http://www.geobase.ca/geobase/en/data/cded/>). These elevation data are derived from provincial and national topographic data sources, and are provided as a 1:50,000 digital elevation model (DEM). The DEM, which has a native spatial resolution of approximately 23 m (0.75 arc seconds), was resampled to match the 30 m spatial resolution of our image composite using bilinear resampling. From the 30 m DEM we calculated slope (in degrees), the Topographic Solar Radiation Index (TRASP; a transformed measure of aspect), and the Topographic Wetness Index (TWI) (Table 3).

### ***Species distribution modeling***

Species distribution modelling was conducted using Random Forests™ (RF) in R 3.1 (Breiman, 2001). We chose RF, a type of decision tree, because it can accommodate non-normal responses and non-linear relationships, and automatically account for interactions among predictors (De'ath and Fabricus, 2000; Elith et al., 2008; Hawkins, 2012). Decision trees involve a sequence of binary splits at values of the predictor variables that result in the maximum differentiation of values of the response variable (in this case, species dominance or non-dominance at a given location). In RF, many (500 to 2000) single trees are developed, each constructed from a different bootstrapped sample of the training data and a randomly selected subset of the predictor variables (Prasad et al., 2006). The predictions are averaged over all trees to generate an overall probability while minimizing the chances of over-fitting to the training data (Franklin, 2009; Prasad et al., 2006). Ensemble tree methods have been found to perform well relative to most other predictive methods across many regions, and species, including plants (Elith et al., 2006; Guisan et al., 2007b; Prasad et al., 2006).

The use of RF for species distribution modeling involved both fitting and prediction stages. First, each model was fit using the species observation data from Table 1 and the mean of each predictor variable. The predictor variables used in the modelling were selected from among the multiple, aforementioned topographic and spectral variables after conducting a Spearman's rank correlation analysis and assessing variable utility through boxplots for each predictor variable across all species. Specifically, we selected the following three spectral and two

topographic indices for use as inputs, all with correlations less than  $\pm 0.15$ : the Tasseled Cap TCG, TCB, and TCW, the TRASP and the TWI (Table 3). We used 500 decision trees, with a random subset of two of the explanatory variables chosen for input for each of these individual trees. Because of the unbalanced number of observations of dominance and non-dominance in the training data for a given species (Table 1), we used a “down-sampling” approach, specifying that each model should use all samples from the least common class (dominance), and an equal number of samples from the more common class (non-dominance) (Chen et al., 2004). A separate RF model was generated for each species, and thus the number of samples varied across models.

Each output RF model contained probabilities of dominance ranging from 0 to 1, which are classified by default into the binary classes dominance or non-dominance, if probabilities are  $\geq 0.5$  or  $< 0.5$ , respectively. However, often a threshold probability other than 0.5 is preferred (Nenzén and Araújo, 2011), particularly for rare species (Freeman and Moisen, 2008). To choose appropriate threshold probabilities for our models, we generated a Receiver Operating Characteristic (ROC) plot for each species using the `auc.roc.plot()` function in the `PresenceAbsence` library in R (v3.1.2). An ROC plot shows how the rate of true positives (y-axis) versus false positives (x-axis) of a model vary for all threshold probabilities between 0 and 1. A perfect classification would pass through the upper left corner of the plot (100% true positives and 0% false positives). A threshold value that achieves the minimal distance between this place of perfect classification and the curve, is an appropriate value to transform continuous outputs to binary classifications (Liu et al., 2005).

Finally, each of the six models were re-run using values of the predictor variables for locations (pixels) where species observations were absent, and the predictions of dominance and non-dominance output as continuous raster surfaces using the determined thresholds. A secondary goal was to create a forest composition map with all species combined. A composite species map was generated by evaluating the individual probabilities of dominance resulting from each of the six RF models were compared at each location (pixel) and that species with the highest overall probability was selected as the appropriate classification value for that location.

### ***Model evaluation***

Model performance was assessed using the *out-of-bag* (OOB) error generated internally by the RF method eliminating the need for a separate cross-validation (Breiman, 2001). Specifically, the ability of the classifier to correctly predict observed values was assessed, where discrete class predictions were based on species-specific probability thresholds determined through the ROC analysis described above. We also examined the Area Under the Curve (AUC) associated with an ROC plot, as calculated by back-predicting on our observed data (essentially but not exactly the same data used for training because of the subsampling and consensus approach used in `RandomForests`). The AUC ranges from 0.5 to 1, and indicates the proportion of times that the model discriminates between our two outcomes better than random (Jiménez-Valverde, 2012), or more specifically, the proportion of times a randomly chosen instance of dominance has a value larger than that for a randomly chosen instance of non-dominance (Fielding and Bell, 1997). Thus higher AUC values indicate better models.

Finally, we compared our resultant tree distribution models with previous studies, general knowledge of the species’ ranges, and trends of dominance per ecozone and ecoregion. In particular, we calculated the areal extent of each dominant species as predicted in our overall forest composition map per ecozone and ecoregion and ranked these in descending order. We

repeated this calculation using homogenous polygons from NFI photo plot data to assess agreement between model outputs and the training data over a broader scale. Similarly, we generated regional summaries of species dominance by combining predictions of relative basal area for the same species from a recent study by Beaudoin et al. (2014).

### ***Assessing the effects of the image composite on spatial patterns of the models***

To assess the impact that compositing had on predicting species distributions, we tested the hypothesis that the spatial pattern of predictions was similar for reference sample blocks and non-reference sample blocks. Reference blocks had pixel observations derived from a single year, a single DOY, and a single sensor, while non-reference blocks had pixel observations from multiple years, DOYs, and sensors. Spatial patterns can be quantified by a combination of composition and configuration. Whereas composition is *aspatial* and refers to the variety and (relative) abundance of different features (e.g., tree species), configuration refers both to the spatial characteristics of individual patches such as size and shape, as well as spatial relationships among neighbouring patches or neighbouring cells (Gustafson, 1998). While composition indicates what is present at any given location, configuration metrics provide a context to local conditions, and permits study of how spatial patterns are an expression of process (Fahrig, 2005; Turner, 1989).

The analysis was undertaken within sample blocks measuring 1020 m x 1020 m, distributed over a random 10% of the study area (for a total of 31,840 samples). An extent of 1020 m x 1020 m was chosen to ensure coverage of the data gaps (of 1 to 14 pixels in size, see Goward et al., 2010; Storey et al., 2005) resulting from Landsat 7 ETM+ Scan-Line Correction failure, while also being a number within which 30 m Landsat pixels could be equally divided. Three image composite characteristics were evaluated: acquisition year (2009, 2010, or 2011), sensor (TM or ETM+), and the number of days from the target DOY of August 1 (ranging from 0 to 30).

For each species, composition was quantified within each 1020 m x 1020 m block as the sum of pixels with predicted dominance for that species. All blocks had dominance of at least one species. Configuration was measured for each species using join counts within each 1020 m x 1020 m area. A join count test can be used to assess spatial autocorrelation in categorical, especially binary, variables, such as dominance/non-dominance (Boots, 2006). Using a join count, the spatial configuration of a species can be quantified as clustered or dispersed, relative to complete spatial randomness (O’Sullivan and Unwin, 2010). For binary data, the two categories are normally referred to as either “Black” (B) or “White” (W) (here, dominance or non-dominance, respectively). For this analysis, we were interested only in the  $J_{BB}$  (dominance-dominance) join-count statistic:

$$J_{BB} = \frac{1}{2} \left( \sum_{i=1}^n \sum_{\substack{j=1 \\ j \neq i}}^n \delta_{ij} x_i x_j \right) \frac{1}{2} \left( \sum_{i=1}^n \sum_{\substack{j=1 \\ j \neq i}}^n \delta_{ij} x_i x_j \right)$$

where  $i$  and  $j$  are the two sampling units being compared,  $x_i$  is the value of the sampling unit (1 or 0), and  $\delta_{ij}$  is the adjacency of  $i$  and  $j$  (1 when they are adjacent, 0 when they are not). The expected values of joins are then calculated based on the proportion of each category and number of total joins in the study (which depends on how connectivity is defined), and the observed and expected values are then compared to assess the null hypothesis of complete spatial randomness (Fortin and Dale, 2005). We computed a join count for each species, using the

Rook's case definition of contiguity (four neighbours). Each species had to be predicted within at least two 30 m cells within each 1020 m x 1020 m block to be included in the analysis. Missing data within each 1020 m x 1020 m block were reclassified as zeroes to allow calculation of the join-counts, while remaining statistically conservative.

To assess whether the use of an image composite affected our modelled species distributions, we compared values of composition and configuration between reference (n = 23,581) and non-reference (n=8259) sample blocks. We calculated the frequency distribution of the composition and configuration values for each of the six species from the reference sample blocks, and extracted the 5<sup>th</sup> and 95<sup>th</sup> percentiles for each. The number of composition and configuration values in the non-reference sample blocks that fell below the 5<sup>th</sup> or above the 95<sup>th</sup> percentiles was then calculated. Blocks with these unexpected values were then mapped and a summary of their sensor type, year and DOY characteristics were extracted.

## RESULTS

### *Species distribution modelling*

The ROC threshold optimization method resulted in a threshold of 0.7 for all species except for *Picea mariana* and *Populus tremuloides*, for which the optimum threshold was 0.6 (Table 4). These thresholds were used to map the distribution of each individual tree species (Figure 3). Combining the individual species maps creates an overall map of forest composition (Figure 4). *Pinus banksiana* was predicted to dominate over the largest spatial extent (8.9 million hectares in total), particularly at mid-to-high latitudes (Figure 4). *Populus tremuloides* was predicted to dominate in the southern extreme of the Boreal Plain ecozone, in the Aspen Parkland ecoregion, but is also found across the province even in the far north, with predicted dominance covering 7.3 million ha in total. *Picea mariana* was predicted to be the next most widespread species, dominating over 6.6 million ha, particularly at mid-latitudes, but being also widespread in the north. *Larix laricina* was predicted to be dominant at low to mid latitudes in the Boreal transition ecoregion and in lowland areas and known wet areas such as the Saskatchewan River delta, straddling the eastern border of Saskatchewan, covering 3.4 million ha in total. *Picea glauca* and *Betula papyrifera* were predicted to dominate with considerably less extent (approximately 1.3 million ha and 824,000 ha respectively).

### *Model evaluation*

The ability of our models to correctly classify the dominance or non-dominance of individual species varied from species to species (Table 4). Overall, OOB error rates were less than 25%, indicating reasonable model fit to the training data. Error rates were much lower for species with sufficient sample sizes. Specifically, at the selected thresholds, *Populus tremuloides* (with one of the highest sample sizes) had the lowest OOB error at 9%. *Betula papyrifera* and *Picea glauca* (with the two lowest sample sizes) had the highest OOB error rates at 24% each. AUC values were very high for all models (0.99 to 1), indicating good model performance.

Trends in the relative areal extent of species dominance for the province's forested ecozones and ecoregions predicted in this study are generally comparable to those in the NFI photo plot database, as well as to those of species occurrence from Beaudoin et al. (2014) (Table 5). For example, all three studies/datasets indicated that both the Boreal Plain Ecozone, and Boreal Transition Ecoregion, are dominated by *Populus tremuloides*. All three datasets also



suggest *Pinus banksiana* is dominant in the Athabasca Plain ecoregion. Some differences are also apparent. For instance, the current study predicts *Pinus banksiana* to be dominant across the largest proportion of the Taiga Shield, whereas the other datasets indicate *Picea mariana* is most dominant.

### ***Assessing the effects of the image composite on spatial patterns of the models***

The proportion of composition and configuration values within the non-reference sample blocks falling outside the expected distribution (5<sup>th</sup> to 95<sup>th</sup> percentiles of values of the reference blocks) was fairly low. Depending on the species, 3.7% to 9.6% of the blocks had unexpected composition values, while 7.1% to 16.5% had unexpected configuration values (Table 6). Given that we set the critical value of the statistical comparison to 0.10, we would expect around 10% of blocks to have unexpected composition and configuration. Only the configuration of *Populus tremuloides* had a higher than statistically expected number of unexpected blocks (16.5%). The spatial distribution of the sample blocks with unexpected composition and configuration values appears random (Figure 5). Further, the DOY, year and sensor characteristics in these expected and unexpected regions were found to be very similar. For instance, all of these non-reference sample blocks, regardless of whether they had expected or unexpected values of species composition and configuration, were comprised primarily of imagery from 2010, with the difference in proportions of 2010 imagery between expected and unexpected blocks ranging from ~2% to 9%, depending on the species. Likewise, all blocks contained imagery primarily from Landsat 5; blocks with unexpected values of composition and configuration differed in terms of sensor composition by no more than 9% from blocks with expected values. Mean DOY differed by no more than two days for blocks with expected and unexpected samples of species composition and configuration.

## **DISCUSSION**

The use of satellite imagery for vegetation mapping is a desirable supplement to ground or photo-based inventories because of the large spatial extents that can be covered by satellite imagery, as well as the associated automated, repeated acquisition. Tree species distribution mapping based on satellite imagery involves the detection or classification of separate spectral reflectance signatures for each species (Bradter et al., 2011); however, tree species classification is difficult, as many vegetation species have overlapping spectral reflectance characteristics in the wavebands collected by typical multispectral sensors (Immitzer et al., 2012; van Aardt and Wynne, 2001). Hyperspectral imagery, which collects reflectance in many, narrow wavebands, is often needed to map species composition to a high, or even modest, degree of accuracy (e.g., Buddenbaum et al., 2005; Ustin and Xiao, 2001). However, this type of imagery is not currently cost effective for inventorying large regions because, like high spatial resolution data, hyperspectral imagery are associated with small spatial extents, requiring multiple scenes or, more likely, airborne collections to represent a given area, thereby increasing data costs and processing overhead. In this study we mapped the probable distribution of dominance of six tree species across a large region using freely available moderate spatial resolution multispectral imagery. Our model error rates (~10-25%) were typical for forest species distribution modeling using this type of imagery (e.g., Evans and Cushman, 2009b).

Some error and uncertainty in our distribution models can be attributed to limited sample size. Sample size of the species data has been shown to affect the accuracy of predictive models

in previous research (Stockwell and Peterson, 2002; Wisz et al., 2008). Although machine learning and ensemble methods like Random Forests can perform relatively well with small to moderate sample sizes, especially when absence information is available in addition to presence information (Elith et al., 2006; Guisan et al., 2007a), estimates of error in this study were nonetheless highest for the species with the lowest sample sizes (Table 1). Model accuracies may have also been affected by characteristics of the individual species modelled. Specifically, wide-ranging species are typically more challenging to model than species with more particular niches (Guisan et al., 2007b; McPherson et al., 2004). The six tree species modelled in this study are all wide-ranging species, and are generally tolerant of a range of soils and parent materials (Farrar, 1995). That our training data indicated where a species was and was not dominant was therefore likely particularly important. Indeed, distribution models are particularly robust when reliable absence data are available in addition to presence data (Brotons et al., 2004).

Another potential source of uncertainty in large area mapping and modelling relates to the remotely sensed data itself. In multi-temporal image analysis, differences in atmospheric conditions, and variability in phenology, sun angle and view angle of imagery (Song and Woodcock, 2003) can lead to some uncertainty. Moreover, relationships between species and image spectral reflectances will vary seasonally according to species phenology (Maeda et al., 2014). In this study, we explored the use of a multi-year BAP composite to generate a series of distribution models for the six most common tree species in the forested area of Saskatchewan. We found that mean acquisition year, DOY, and sensor were similar regardless of the level of local complexity found in the composite. In other words, the variability of image characteristics across the BAP composite was actually very small, which was achievable due to the vast archive of open-source Landsat imagery (White and Wulder, 2013), the rules used for compositing, and the pre-processing applied that converted the data to surface reflectance (White et al., 2014).

Composition and configuration of the predicted species are important characteristics to consider in species distribution modelling because spatial pattern is an expression of underlying spatial processes (Nelson and Boots, 2008). Spatial pattern analysis is used to assess model error as it allows patterns in error or uncertainty to be detected and enables departures from random noise to be determined (Wulder et al., 2007). The approach used in this study allows mapping and detection of statistical departures in patterns of species distributions generated from non-reference imagery (Nelson and Boots, 2005). We found that in all but one instance (*Populus tremuloides*) the composition and configuration of species distributions was not different among sample blocks with variable composite characteristics. This species in particular may stand out from the rest simply due to its overall prominence across the study area. Nonetheless, as the majority of our models were unaffected by the compositing, we are confident that the compositing rules used relating to sensor type, target DOY and cloud contamination minimized illumination and phenological differences sufficiently across space. Overall, results indicate that the relation between predicted species distributions and important environmental processes are represented, rather than species spatial pattern being the result of data artifacts in the composite. Overall, our individual maps of the probable distribution of tree species dominance across Saskatchewan meet expected trends as captured through two other independent data sources. For instance, broad-leaved species *Populus tremuloides* and *Betula papyrifera* were predicted to be dominant over a greater spatial extent in the south, relative to the north. The species predicted to be most widespread were *Picea mariana*, *Pinus banksiana*, and *Populus tremuloides*. These three species are typically dominant over a large number of ecosites in the province

(McLaughlan et al., 2010). The primary difference among the three datasets is this study's predicted dominance of *Pinus banksiana* in the Taiga Shield, versus the dominance of *Picea mariana* in this region in the other datasets. We note that there are very few NFI plots in this ecozone, however, and that the differences between our results and those of Beaudoin et al. (2014) likely stem from the use of different remotely sensed data (MODIS) with a different spatial resolution (250 m), and a different modelling approach (kNN).

## CONCLUSION

Regional-scale, spatially comprehensive maps of forest composition have traditionally been limited by the mismatch between desired, versus available, spatial extent and spatial resolution of data. In this analysis, we have demonstrated the capacity to use 30 m Landsat data to map detailed tree species distributions over large areas, by capitalizing on archived, multi-temporal imagery composited using the BAP approach (White et al., 2014). The variability introduced by the BAP compositing was found to be minimal, and resulted in mostly insignificant differences in this large-area mapping application. Future applications will benefit from analyses of the effects of BAP compositing in other geographic regions and for features of interest other than tree species. The potential of the BAP approach to provide source data for developing species distribution maps over large areas will continue to increase with Landsat continuity and the launch of complementary satellites such as Sentinel-2 in 2015 (Drusch et al., 2012; Roy et al., 2014). The constellations of these new satellites have been designed such that, taken together, the majority of the Earth will be able to be imaged twice weekly (Wulder and Coops, 2014) at a 30 m spatial resolution. Spatially continuous maps of tree species distributions over large areas will be useful for a variety of information needs, including forest management, carbon modeling, ecosystem service assessment, and conservation planning.

## ACKNOWLEDGEMENTS

This research was undertaken as part of the “National Terrestrial Ecosystem Monitoring System (NTEMS): Timely and detailed national cross-sector monitoring for Canada” project jointly funded by the Canadian Space Agency (CSA) Government Related Initiatives Program (GRIP) and the Canadian Forest Service (CFS) of Natural Resources Canada. Additional funding provided by The Natural Sciences and Engineering Research Council of Canada (NSERC). Three anonymous reviewers are thanked for their insights and constructive suggestions that served to improve this manuscript.

## REFERENCES

- Beaudoin, A., Bernier, P.Y., Guindon, L., Villemaire, P., Guo, X.J., Stinson, G., Bergeron, T., Magnussen, S., Hall, R.J., 2014. Mapping attributes of Canada's forests at moderate resolution through k NN and MODIS imagery. *Can. J. For. Res.* 44, 521–532.
- Beven, K.J., Kirkby, M.J., 1979. A physically based, variable contributing area model of basin hydrology. *Hydrol. Sci. Bull.* 24, 43–69.
- Boots, B., 2006. Local configuration measures for categorical spatial data: binary regular lattices. *J. Geogr. Syst.* 8, 1–24.

- Bradter, U., Thom, T.J., Altringham, J.D., Kunin, W.E., Benton, T.G., 2011. Prediction of National Vegetation Classification communities in the British uplands using environmental data at multiple spatial scales, aerial images and the classifier random forest. *J. Appl. Ecol.* 48, 1057–1065.
- Breiman, L., 2001. Random Forests. *Mach. Learn.* 45, 5–32.
- Brotons, L., Thuiller, W., Araújo, M., Hirzel, A., 2004. Presence-absence versus presence-only modelling methods for predicting bird habitat suitability. *Ecography (Cop.)*. 27, 437–448.
- Buddenbaum, H., Schlerf, M., Hill, J., 2005. Classification of coniferous tree species and age classes using hyperspectral data and geostatistical methods. *Int. J. Remote Sens.* 26, 5453–5465.
- Chen, C., Liaw, A., Breiman, L., 2004. Using random forest to learn imbalanced data. Technical Report 666.
- Coops, N.C., Waring, R.H., 2010. A process-based approach to estimate lodgepole pine (*Pinus contorta* Dougl.) distribution in the Pacific Northwest under climate change. *Clim. Change* 105, 313–328.
- Crist, E.P., 1985. A TM tasseled cap equivalent transformation for reflectance factor data. *Remote Sens. Environ.* 17, 301–306.
- Crist, E.P., Cicone, R.C., 1984. A Physically-based transformation of Thematic Mapper data - the TM Tasseled Cap. *IEEE Trans. Geosci. Remote Sens.* GE-22, 256–263.
- Crist, E.P., Laurin, R., Cicone, R.C., 1986. Vegetation and soils information contained in transformed Thematic Mapper data, in: *Proceedings of IGARSS' 86 Symposium*. ESA SP-254. European Space Agency, Paris, France, pp. 1465–70.
- De'ath, G., Fabricus, K.E., 2000. Classification and Regression Trees: a powerful yet simple technique for ecological data analysis. *Ecology* 81, 3178–3192.
- Defries, R., Hansen, M., Townshend, J., 1995. Global discrimination of land cover types from metrics derived from AVHRR Pathfinder data. *Remote Sens. Environ.* 54, 209–222.
- Drusch, M., Del Bello, U., Carlier, S., Colin, O., Fernandez, V., Gascon, F., Hoersch, B., Isola, C., Laberinti, P., Martimort, P., Meygret, A., Spoto, F., Sy, O., Marchese, F., Bargellini, P., 2012. Sentinel-2: ESA's optical high-resolution mission for GMES operational services. *Remote Sens. Environ.* 120, 25–36.
- Ecological Stratification Working Group, 1996. A National Ecological Framework for Canada. Ottawa/Hull. Agriculture and Agri-Food Canada, Research Branch, Centre for Land and Biological Resources Research, and Environment Canada, State of the Environment Directorate, Ecozone Analysis Branch.

- Elith, J., Graham, C., Anderson, R., Dudik, M., Ferrier, S., Guisan, A., Hijmans, R., Huettmann, F., Leathwick, J.R., Lehmann, A., Li, J., Lohmann, L., Loiselle, B., Manion, G., Moritz, C., Nakamura, M., Nakazawa, Y., Overton, J.M., Tonwsend, A., Phillips, S.J., Richardson, K.S., Scachetti-Pereira, R., Schaprie, R., Soberon, J., Williams, S., Wisz, M., Zimmermann, N.E., 2006. Novel methods improve prediction of species' distributions from occurrence data. *Ecography (Cop.)*. 29, 129–151.
- Elith, J., Leathwick, J.R., Hastie, T., 2008. A working guide to boosted regression trees. *J. Anim. Ecol.* 77, 802–13.
- Evans, J.S., Cushman, S.A., 2009. Gradient modeling of conifer species using random forests. *Landsc. Ecol.* 24, 673–683.
- Fahrig, L., 2005. When is a landscape perspective important?, in: Wiens, J., Moss, M. (Eds.), *Issues and Perspectives in Landscape Ecology*. Cambridge University Press, Cambridge UK, pp. 3–10.
- Falkowski, M.J., Wulder, M.A., White, J.C., Gillis, M.D., 2009. Supporting large-area, sample-based forest inventories with very high spatial resolution satellite imagery. *Prog. Phys. Geogr.* 33, 403–423.
- Farrar, J., 1995. *Trees in Canada*. Fitzhenry and Whiteside Ltd.
- Fielding, A.H., Bell, J.F., 1997. A review of methods for the assessment of prediction errors in conservation presence/absence models. *Environ. Conserv.* 24, 38–49.
- Fleishman, E., Noss, R., Noon, B., 2006. Utility and limitations of species richness metrics for conservation planning. *Ecol. Indic.* 6, 543–553.
- Fortin, M.-J., Dale, M., 2005. *Spatial analysis: A guide for ecologists*. Cambridge University Press.
- Franklin, J., 2009. *Mapping species distributions: spatial inference and prediction*. Cambridge University Press, Cambridge UK.
- Freeman, E.A., Moisen, G.G., 2008. A comparison of the performance of threshold criteria for binary classification in terms of predicted prevalence and kappa. *Ecol. Modell.* 217, 48–58.
- García Márquez, J.R., Dormann, C.F., Sommer, J.H., Schmidt, M., Thiombiano, A., Da, S.S., Chatelain, C., Dressler, S., 2012. A methodological framework to quantify the spatial quality of biological databases. *Biodivers. Ecol.* 4, 25–39.
- Gillis, M.D., Omule, A.Y., Brierley, T., 2005. Monitoring Canada's forests: The National Forest Inventory. *For. Chron.* 81, 214–221.

- Goward, S., Williams, D., Arvidson, T., Irons, J., 2010. The future of Landsat-class remote sensing, in: Ramachandran, B., Justice, C.O., Abrams, M. (Eds.), *Land Remote Sensing and Global Environmental Change: NASA's Earth Observing System and the Science of ASTER and MODIS*. Springer.
- Griffiths, P., Kuemmerle, T., Baumann, M., Radeloff, V.C., Abrudan, I. V., Lieskovsky, J., Munteanu, C., Ostapowicz, K., Hostert, P., 2014. Forest disturbances, forest recovery, and changes in forest types across the Carpathian ecoregion from 1985 to 2010 based on Landsat image composites. *Remote Sens. Environ.* 151, 72–88.
- Griffiths, P., Linden, S. Van Der, Kuemmerle, T., Hostert, P., 2013. A pixel-based Landsat compositing algorithm for large area land cover mapping. *IEEE J. Sel. Top. Appl. Earth Obs. Remote Sens.* 1–14.
- Guisan, A., Graham, C., Elith, J., Huettmann, F., 2007a. Sensitivity of predictive species distribution models to change in grain size. *Divers. Distrib.* 13, 332–340.
- Guisan, A., Zimmermann, N.E., Elith, J., Graham, C.H., Phillips, S.J., Peterson, A.T., 2007b. What matters for predicting the occurrences of trees: techniques, data, or species' characteristics? *Ecol. Monogr.* 77, 615–630.
- Gustafson, E.J., 1998. Quantifying landscape spatial pattern: What is the state of the art? *Ecosystems* 1, 143–156.
- Hamann, A., Wang, T., 2006. Potential effects of climate change on ecosystem and tree species distribution in British Columbia. *Ecology* 87, 2773–2786.
- Hansen, M.J., Franklin, S.E., Woudsma, C., Peterson, M., 2001. Forest Structure Classification in the North Columbia Mountains Using the Landsat TM Tasseled Cap Wetness Component. *Can. J. Remote Sens.* 27, 20–32.
- Hawkins, B.A., 2012. Eight (and a half) deadly sins of spatial analysis. *J. Biogeogr.* 39, 1–9.
- Hortal, J., Lobo, J.M., Jiménez-Valverde, A., 2007. Limitations of biodiversity databases: case study on seed-plant diversity in Tenerife, Canary Islands. *Conserv. Biol.* 21, 853–863.
- Immitzer, M., Atzberger, C., Koukal, T., 2012. Tree species classification with Random Forest using very high spatial resolution 8-band WorldView-2 satellite data. *Remote Sens.* 4, 2661–2693.
- Jetz, W., Sekercioglu, C.H., Watson, J.E.M., 2007. Ecological correlates and conservation implications of overestimating species geographic ranges. *Conserv. Biol.* 22, 110–119.
- Jiménez-Valverde, A., 2012. Insights into the area under the receiver operating characteristic curve (AUC) as a discrimination measure in species distribution modelling. *Glob. Ecol. Biogeogr.* 21, 498–507.

- Kauth, R., Thomas, G., 1976. The tasselled cap - a graphic description of the spectral-temporal development of agricultural crops as seen by Landsat, in: LARS Symposia, Paper 159.
- Key, C.H., Benson, N.C., 2006. Landscape Assessment (LA) Sampling and Analysis Methods, in: FIREMON: Fire Effects Monitoring and Inventory System. USDA Forest Service Gen. Tech. Rep. RMRS-GTR-164-CD: LA 1-51, Rocky Mountain Research Station, Ogden, UT.
- Kremen, C., 2005. Managing ecosystem services: what do we need to know about their ecology? *Ecol. Lett.* 8, 468–79.
- Little, E.L. Jr., 1971. Atlas of United States trees, volume 1, conifers and important hardwoods: U.S. Department of Agriculture Miscellaneous Publication 1146.
- Liu, C., Berry, P.M., Dawson, T.P., Pearson, R.G., 2005. Selecting thresholds of occurrence in the prediction of species distributions 3, 385–393.
- Loveland, T.R., Merchant, J.W., Ohlen, D.O., Brown, J.F., 1991. Development of a Land-Cover Characteristics Database for the Conterminous U.S. *Photogramm. Eng. Remote Sens.* 57, 1453–1463.
- Maeda, E.E., Heiskanen, J., Thijs, K.W., Pellikka, P.K.E., 2014. Season-dependence of remote sensing indicators of tree species diversity. *Remote Sens. Lett.* 5, 404–412.
- McLaughlan, M.S., Wright, R.A., Jiricka, R.D., 2010. Field guide to the Ecosites of Saskatchewan's Provincial Forests.
- McPherson, J., Jetz, W., Rogers, D., 2004. The effects of species' range sizes on the accuracy of distribution models: ecological phenomenon or statistical artefact? *J. Appl. Ecol.* 41, 811–823.
- McPherson, J.M., Jetz, W., 2007. Type and spatial structure of distribution data and the perceived determinants of geographical gradients in ecology: the species richness of African birds. *Glob. Ecol. Biogeogr.* 16, 657–667.
- Moisen, G.G., Freeman, E.A., Blackard, J.A., Frescino, T.S., Zimmermann, N.E., Edwards, T.C., 2006. Predicting tree species presence and basal area in Utah: A comparison of stochastic gradient boosting, generalized additive models, and tree-based methods. *Ecol. Modell.* 199, 176–187.
- Natural Resources Canada, 2010. Canadian National Fire Database - agency fire data.
- Nelson, T.A., Boots, B., 2005. Identifying insect infestation hot spots: an approach using conditional spatial randomization. *J. Geogr. Syst.* 7, 291–311.
- Nelson, T.A., Boots, B., 2008. Detecting spatial hot spots in landscape ecology. *Ecography (Cop.)*. 31, 556–566.

- Nenzén, H.K., Araújo, M.B., 2011. Choice of threshold alters projections of species range shifts under climate change. *Ecol. Modell.* 222, 3346–3354.
- O’Sullivan, D., Unwin, D., 2010. Area Objects and Spatial Autocorrelation, in: *Geographic Information Analysis*. John Wiley & Sons, Hoboken, New Jersey.
- Pastor, J., Mladenoff, D.J., Haila, Y., Bryant, J., Payette, S., 1996. Biodiversity and Ecosystem Processes in Boreal Regions, in: Mooney, H.A., Cushman, J.H., Medina, E., Sala, O.E., Schulze, E.-D. (Eds.), *Functional Roles of Biodiversity: A Global Perspective*. Wiley.
- Pfeifer-Meister, L., Bridgham, S.D., Little, C.J., Reynolds, L.L., Goklany, M.E., Johnson, B.R., 2013. Pushing the limit: experimental evidence of climate effects on plant range distributions. *Ecology* 94, 2131–2137.
- Prasad, A.M., Iverson, L.R., Liaw, A., 2006. Newer Classification and Regression Tree techniques: bagging and random forests for ecological prediction. *Ecosystems* 9, 181–199.
- Roberts, D.W., Cooper, S.V., 1989. Concepts and techniques of vegetation mapping, in: *Land Classifications Based on Vegetation: Applications for Resource Management*. USDA Forest Service GTR INT-257, Ogden, UT, pp. 90–96.
- Roy, D.P., Ju, J., Kline, K., Scaramuzza, P.L., Kovalskyy, V., Hansen, M., Loveland, T.R., Vermote, E., Zhang, C., 2010. Web-enabled Landsat Data (WELD): Landsat ETM+ composited mosaics of the conterminous United States. *Remote Sens. Environ.* 114, 35–49.
- Roy, D.P., Wulder, M.A., Loveland, T.R., C.E., W., Allen, R.G., Anderson, M.C., Helder, D., Irons, J.R., Johnson, D.M., Kennedy, R., Scambos, T.A., Schaaf, C.B., Schott, J.R., Sheng, Y., Vermote, E.F., Belward, A.S., Bindschadler, R., Cohen, W.B., Gao, F., Hipple, J.D., Hostert, P., Huntington, J., Justice, C.O., Kilic, A., Kovalskyy, V., Lee, Z.P., Lymburner, L., Masek, J.G., McCorkel, J., Shuai, Y., Trezza, R., Vogelmann, J., Wynne, R.H., Zhu, Z., 2014. Landsat-8: Science and product vision for terrestrial global change research. *Remote Sens. Environ.* 145, 154–172.
- Running, S., Loveland, T., Pierce, L., 1994. A vegetation classification logic based on remote sensing for use in global biogeochemical models. *Ambio* 23, 77–81.
- Saskatchewan Environment - Forest Service, 2004. Saskatchewan Forest Vegetation Inventory - Forest Planning Manual, Version 4.0.
- Saskatchewan Ministry of Environment, 2009. Saskatchewan’s 2009 State of the Environment Report.
- Song, C., Schroeder, T., Cohen, W., 2007. Predicting temperate conifer forest successional stage distributions with multitemporal Landsat Thematic Mapper imagery. *Remote Sens. Environ.* 106, 228–237.



- Song, C., Woodcock, C., 2003. Monitoring forest succession with multitemporal Landsat images: factors of uncertainty. *IEEE Trans. Geosci. Remote Sens.* 41, 2557–2567.
- Stockwell, D.R., Peterson, A.T., 2002. Effects of sample size on accuracy of species distribution models. *Ecol. Modell.* 148, 1–13.
- Storey, J., Scaramuzza, P., Schmidt, G., Barsi, J., 2005. Landsat 7 Scan Line Corrector-Off Gap-Filled Product Development, in: *Proceedings from 16th William T. Pecora Memorial Symposium: Global Priorities in Land Remote Sensing*. Oct 23-27, 2005, Sioux Falls, South Dakota.
- Thuiller, W., Lavorel, S., Araújo, M.B., Sykes, M.T., Prentice, I.C., 2005. Climate change threats to plant diversity in Europe. *Proc. Natl. Acad. Sci. U. S. A.* 102, 8245–50.
- Turner, M., 1989. Landscape ecology: the effect of pattern on process. *Annu. Rev. Ecol. Syst.* 20, 171–197.
- Ustin, S.L., Xiao, Q.F., 2001. Mapping successional boreal forests in interior central Alaska. *Int. J. Remote Sens.* 22, 1779–1797.
- Van Aardt, J.A.N., Wynne, R.H., 2001. Spectral Separability among Six Southern Tree Species. *Photogramm. Eng. Remote Sensing* 67, 1367–1375.
- Verbyla, D.L., Hammond, T.O., 1995. Conservative bias in classification accuracy assessment due to pixel- by-pixel comparison of classified images with reference grids. *Int. J. Remote Sens.* 16, 581–587.
- White, J.C., Wulder, M.A., 2013. The Landsat observation record of Canada: 1972 – 2012. *Can. J. Remote Sens.* 39, 455–467.
- White, J.C., Wulder, M.A., Hobart, G.W., Luther, J.E., Hermosilla, T., Griffiths, P., Coops, N.C., Hall, R.J., Hostert, P., Dyk, A., Guindon, L., 2014. Pixel-based image compositing for large-area dense time series applications and science. *Can. J. Remote Sens.* 43, 192–212.
- Wisz, M.S., Hijmans, R.J., Li, J., Peterson, A.T., Graham, C.H., Guisan, A., 2008. Effects of sample size on the performance of species distribution models. *Divers. Distrib.* 14, 763–773.
- Woodcock, C., Allen, R., Anderson, M., Belward, A., Bindschadler, R., Cohen, W., Gao, F., Goward, S.N., Helder, D., Hlemer, E., Nemani, R., Oreopoulos, L., Schott, J., Thenkabail, P., Vermote, E., Vogelmann, J., Wulder, M.A., Wynne, R., 2008. Free access to Landsat imagery. *Science* (80- ). 320, 1011–1012.
- Wulder, M.A., Coops, N.C., 2014. Make Earth observations open access. *Nature* 513, 30–31.

- Wulder, M.A., Hall, R.J., Coops, N.C., Franklin, S.E., 2004a. High Spatial Resolution Remotely Sensed Data for Ecosystem Characterization. *Bioscience* 54, 511–521.
- Wulder, M.A., Kurz, W.A., Gillis, M., 2004b. National level forest monitoring and modeling in Canada. *Prog. Plann.* 61, 365–381.
- Wulder, M.A., Masek, J.G., Cohen, W.B., Loveland, T.R., Woodcock, C.E., 2012. Opening the archive: How free data has enabled the science and monitoring promise of Landsat. *Remote Sens. Environ.* 122, 2–10.
- Wulder, M.A., Skakun, R.S., Kurz, W.A., White, J.C., 2004c. Estimating time since forest harvest using segmented Landsat ETM+ imagery. *Remote Sens. Environ.* 93, 179–187.
- Wulder, M.A., White, J.C., Coops, N.C., Nelson, T.A., Boots, B., 2007. Using local spatial autocorrelation to compare outputs from a forest growth model. *Ecol. Modell.* 209, 264–276.
- Zimmermann, N.E., Edwards, T.C., Moisen, G.G., Frescino, T.S., Blackard, J.A., 2007. Remote sensing-based predictors improve distribution models of rare, early successional and broadleaf tree species in Utah. *J. Appl. Ecol.* 44, 1057–1067.

**Table 1. Species modelled, area and number of National Forest Inventory Photo Plot (NFI PP) polygons dominated by each**

English Name	Latin Name	Dominant (present at $\geq 90\%$ abundance) <sup>a</sup>		Non-Dominant (present at $\leq 10\%$ abundance) <sup>a</sup>
		Number of polygons	Area (km <sup>2</sup> )	Number of polygons
White birch	<i>Betula papyrifera</i>	29	0.71	5404
Tamarack	<i>Larix laricina</i>	459	27.11	4974
White spruce	<i>Picea glauca</i>	49	0.73	5348
Black spruce	<i>Picea mariana</i>	2057	55.81	3376
Jack pine	<i>Pinus banksiana</i>	856	38.63	4577
Trembling aspen	<i>Populus tremuloides</i>	1983	88.48	3450

<sup>a</sup> Count follows exclusion of very small polygons (less than 900 m<sup>2</sup>) and those that were burned or harvested in the time since the polygon was delineated and attributed.

**Table 2. Number of Landsat images used in Best-Available-Pixel composite for Saskatchewan, Canada.**

<b>Year</b>	<b>Candidate*</b>			<b>Composite</b>		
	<b>TM</b>	<b>ETM+</b>	<b>Total</b>	<b>TM</b>	<b>ETM+</b>	<b>Total</b>
<b>2009</b>	379	328	707	345	188	533
<b>2010</b>	362	367	729	342	284	626
<b>2011</b>	406	398	804	333	218	551

\*Candidate images are  $\pm 30$  days of August 1 with less than 70% cloud cover.

**Table 3. Predictor variables used in the Random Forests models of individual tree species distributions.**

<b>Name</b>	<b>Description</b>	<b>Rationale</b>
Brightness		TC brightness can differentiate between soil and vegetated surfaces (Crist et al., 1986) and can help differentiate among successional stages / stand age (Song et al., 2007).
Greenness	Tasseled Cap components (Crist and Cicone, 1984; Crist, 1985)	Greenness in relates to biomass and vegetation vigor and is highly correlated to the Normalized Difference Vegetation Index (NDVI), which is useful for general land cover classification (Defries et al., 1995; Running et al., 1994)
Wetness		TC Wetness correlated to structural complexity (Hansen et al., 2001), perhaps particularly for successional stages / stand age (Wulder et al., 2004c).
Topographic Wetness Index (TWI)	Model of potential surface moisture, based on topographic position (Beven and Kirkby, 1979): $Ln(\text{specific catchment area} / \tan(\text{slope in radians}))$	Soil moisture directly affects plant growth.
Topographic Solar Radiation Aspect Index (TRASP)	Values range from 0 to 1, with 0 indicating cool, NE slopes, and 1 indicating warm SW slopes (Roberts and Cooper, 1989).	Solar radiation affects soil moisture and heat load, and directly affects plant growth.

**Table 4. Threshold used to translate probabilities of species dominance to a binary dominant or non-dominant variable. The threshold selected minimized the distance on a plot of the ROC (Receiver Operating Characteristic) curve between the upper left corner of the plot and the curve.**

<b>Species</b>	<b>Threshold used to create binary map<sup>a</sup></b>	<b>OOB error rate<sup>b</sup> (for class “dominant”)</b>	<b>Area Under the Curve (AUC)<sup>c</sup></b>
<i>Betula papyrifera</i>	0.7	0.24	0.99
<i>Larix laricina</i>	0.7	0.12	0.99
<i>Picea glauca</i>	0.7	0.24	0.99
<i>Picea mariana</i>	0.6	0.11	1
<i>Pinus banksiana</i>	0.7	0.14	1
<i>Populus tremuloides</i>	0.6	0.09	1

<sup>a</sup> According to the criteria of minimizing the distance on a plot of the ROC (Receiver Operating Characteristic) curve between the upper left corner of the plot and the curve.

<sup>b</sup> The Out of Bag (OOB) error indicates the total number of misclassified data points from within the out-of-bag sample (Breiman, 2001).

<sup>c</sup> Values close to 1 indicate good model fit

**Table 5. Spatial Extent of Dominant Tree Species in Saskatchewan’s Forested Ecozones and Ecoregions.**

		<b>Most Spatially Expansive Species</b>		
<b>Ecozone</b>	<b>Ecoregion</b>	<b>NFI photo plot data<sup>1</sup></b>	<b>Beudoin et al. 2014<sup>2</sup></b>	<b>This study</b>
Taiga Shield		<i>Picea mariana</i> (70% of ecoregion)	<i>Picea mariana</i> (80% of ecoregion)	<i>Pinus banksiana</i> (61% of ecoregion)
	Tazin Lake Upland	<i>Picea mariana</i>	<i>Picea mariana</i>	<i>Pinus banksiana</i>
	Selwyn Lake Upland	<i>Picea mariana</i>	<i>Picea mariana</i>	<i>Pinus banksiana</i>
Boreal Shield		<i>Pinus banksiana</i> (48% of ecoregion)	<i>Picea mariana</i> (49% of ecoregion)	<i>Pinus banksiana</i> (46% of ecoregion)
	Athabasca Plain	<i>Pinus banksiana</i>	<i>Pinus banksiana</i>	<i>Pinus banksiana</i>
	Churchill River Upland	<i>Picea mariana</i>	<i>Picea mariana</i>	<i>Pinus banksiana</i>
Boreal Plain		<i>Populus tremuloides</i> (48% of ecoregion)	<i>Populus tremuloides</i> (48% of ecoregion)	<i>Populus tremuloides</i> (40% of ecoregion)
	Mid-Boreal Uplands	<i>Populus tremuloides</i>	<i>Picea mariana</i>	<i>Picea mariana</i>
	Boreal Transition	<i>Populus tremuloides</i>	<i>Populus tremuloides</i>	<i>Populus tremuloides</i>
	Mid-Boreal Lowlands	<i>Larix laricina</i>	<i>Picea mariana</i>	<i>Larix laricina</i>

<sup>1</sup> Calculations included only homogenous polygons (those where  $\geq 90\%$  of the polygon is comprised of a single species).

<sup>2</sup> As in the generation of our forest composition map, each individual species distribution map from Beudoin et al. 2014 was combined and assigned the value of the species with the highest predicted relative basal area. Calculations in this table are based on the combined map.

**Table 6. Proportion of composition and configuration values within non-reference sample blocks (n=8259)\* that are <5<sup>th</sup> or >95<sup>th</sup> percentile of values within reference sample blocks (n=23,581).**

	<i>Betula papyrifera</i>	<i>Larix laricina</i>	<i>Picea glauca</i>	<i>Picea mariana</i>	<i>Pinus banksiana</i>	<i>Populus tremuloides</i>
True sample size*	6177	7361	5588	7966	7446	7675
% unexpected						
<b>Composition</b>	3.71	9.96	5.71	9.63	7.13	8.33
True sample size*	4469	6517	4274	7682	6677	7481
% unexpected						
<b>Configuration</b>	7.14	9.56	7.25	8.69	8.62	16.53

\*note that the non-reference sample size was less than 8259 for each species because for each species in turn, blocks had to contain at least one pixel of presence (dominance) for analysis of composition, and at least two pixels of presence (dominance) for analysis of configuration.



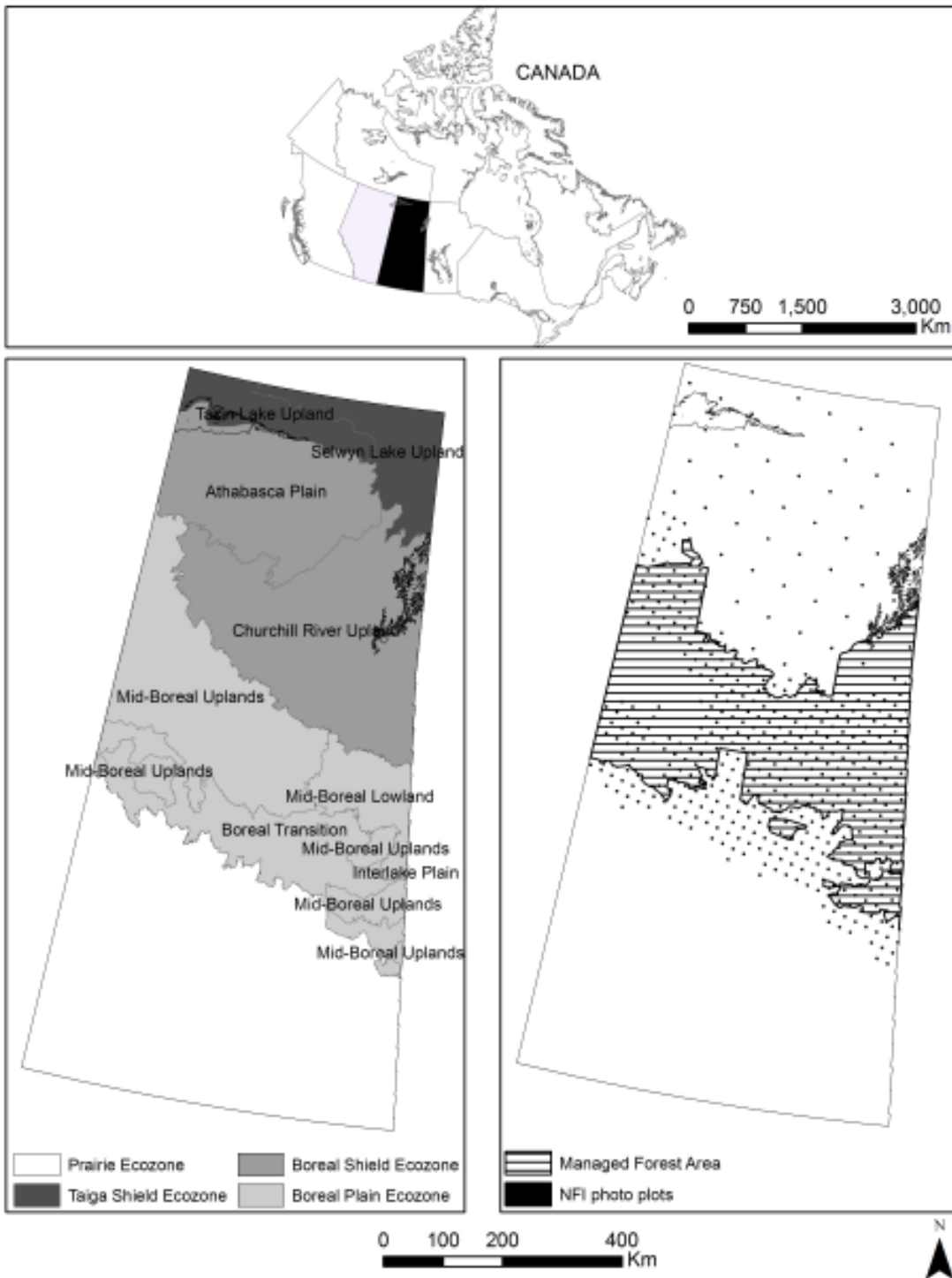


Figure 1. Study area. (a) The province of Saskatchewan (highlighted in black), in central Canada. (b) The forested ecozones and ecoregions of Saskatchewan. (c) The distribution of Canada's National Forest Inventory 2 km x 2 km photo plots across Saskatchewan, including inside and outside of the Managed Forest Area. These inventory data were the source of the training data used to model tree species distributions.

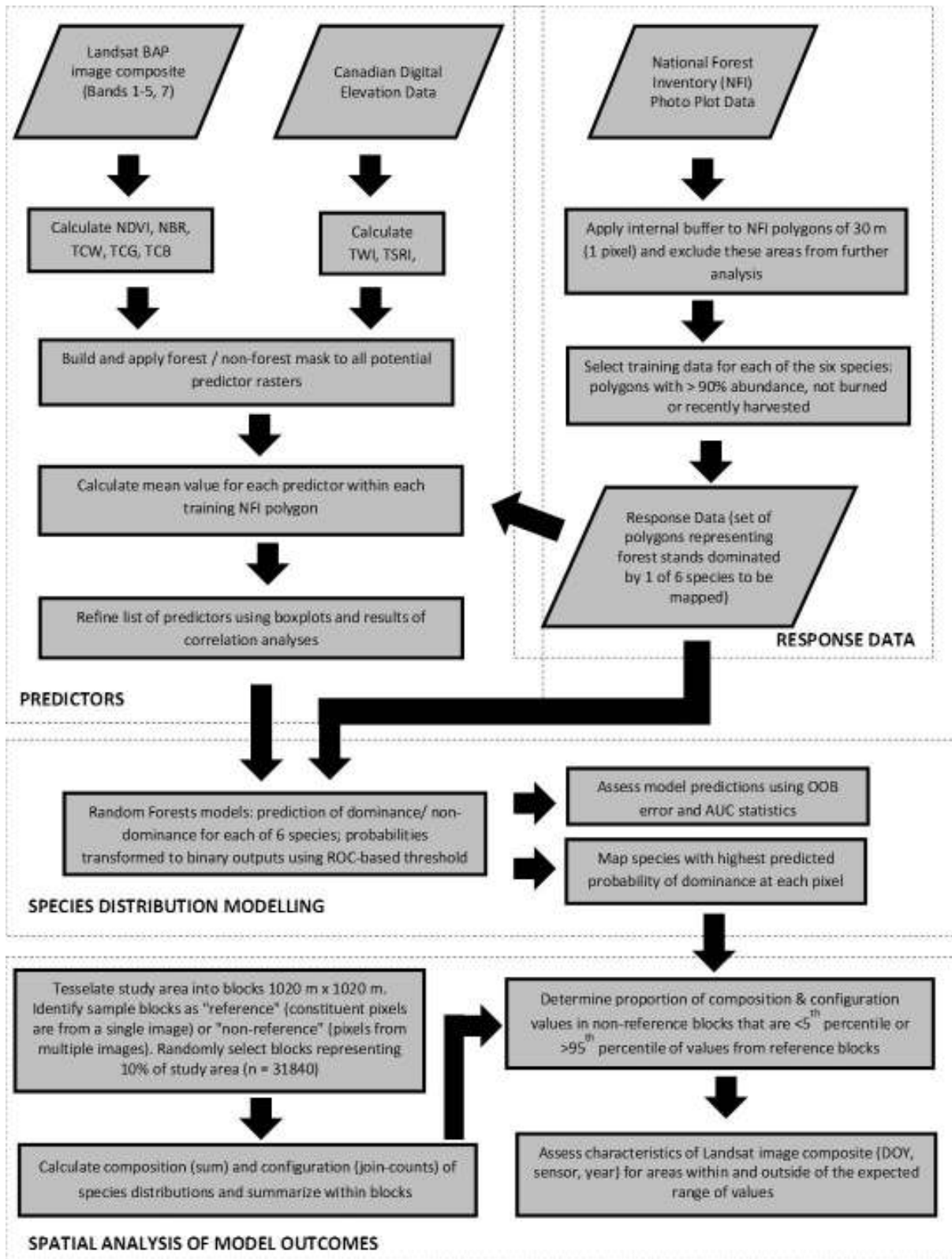


Figure 2. Flowchart of the data and methods followed to model species distributions and assess the impact of BAP composites of the resultant maps.

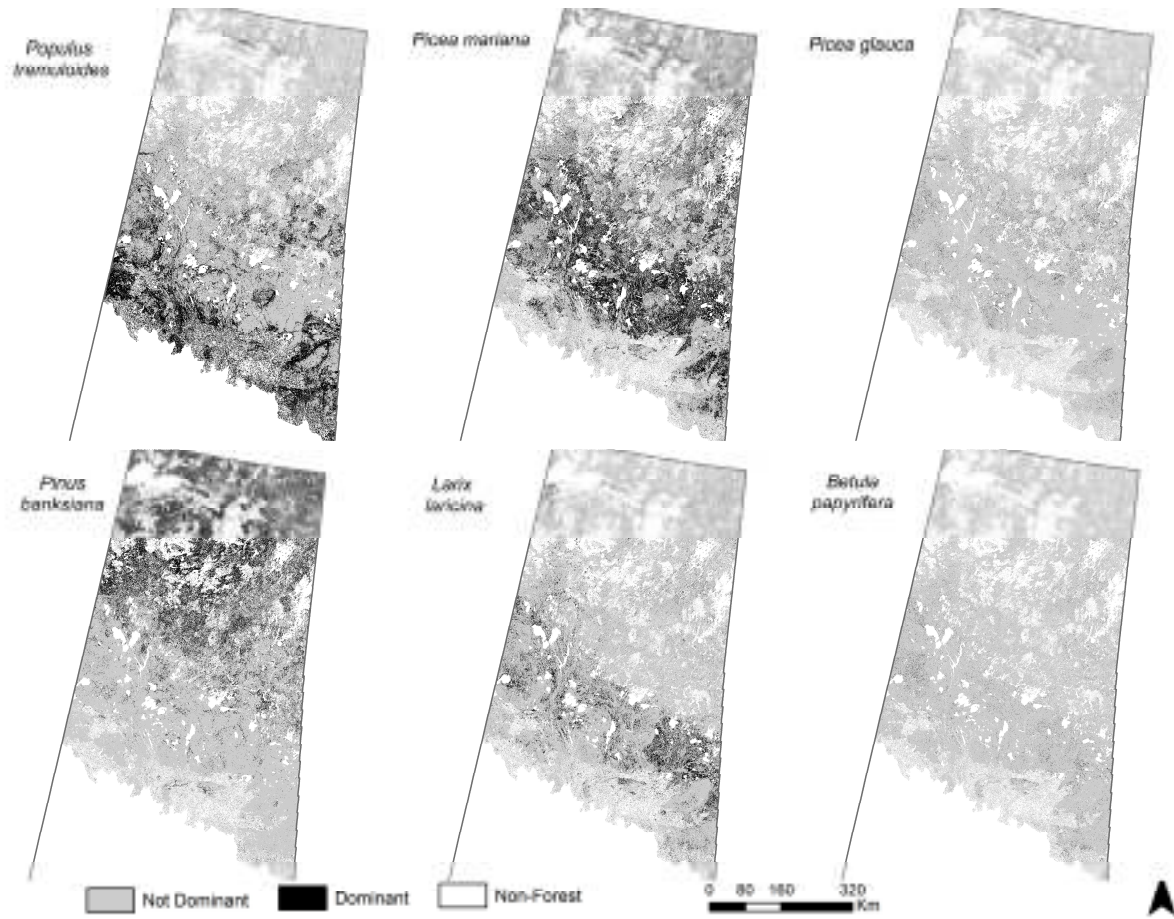


Figure 3. Individual models of tree species dominance in Saskatchewan.

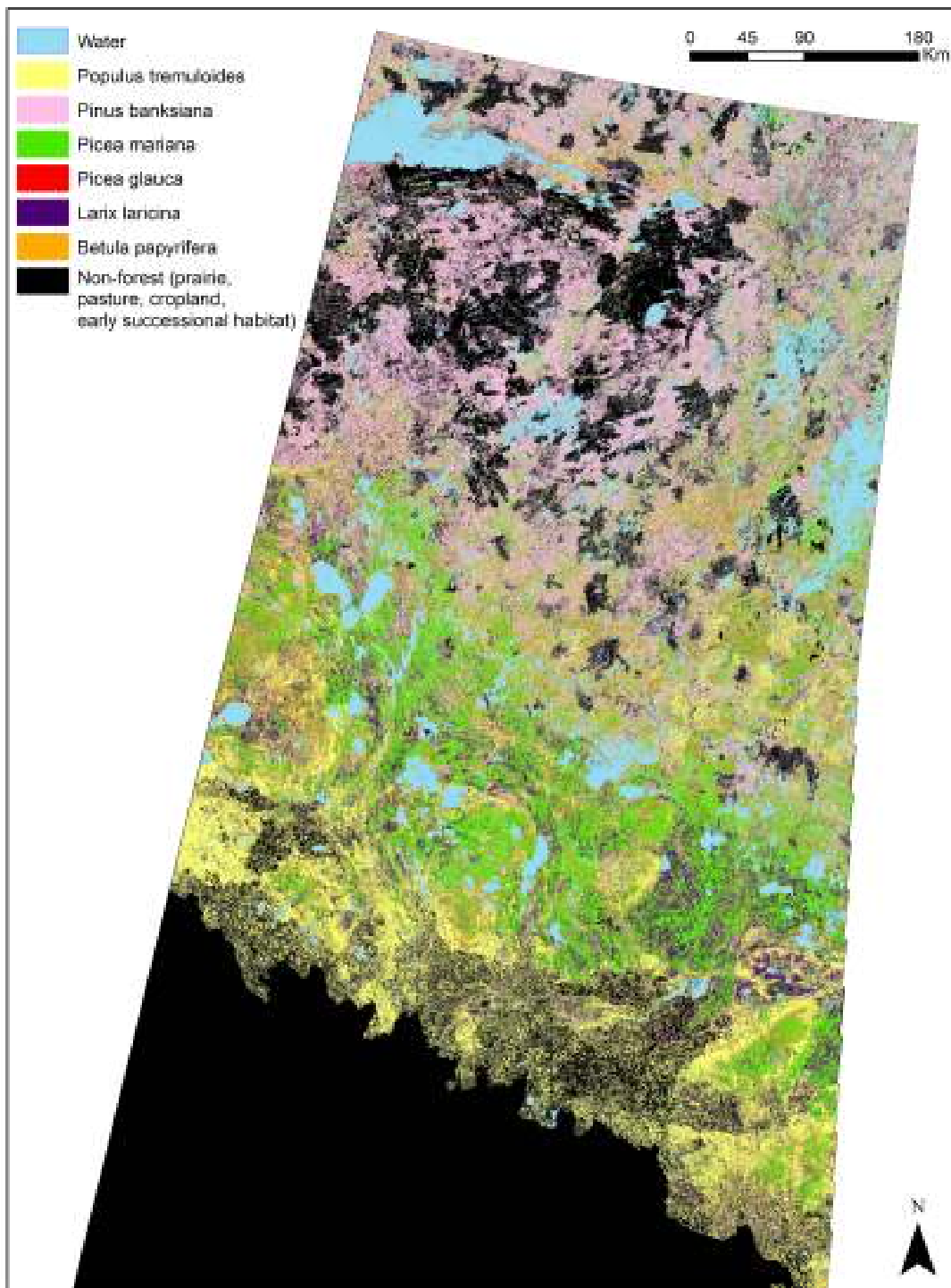


Figure 4. Forest composition map showing tree species with highest predicted probability of dominance at each location.

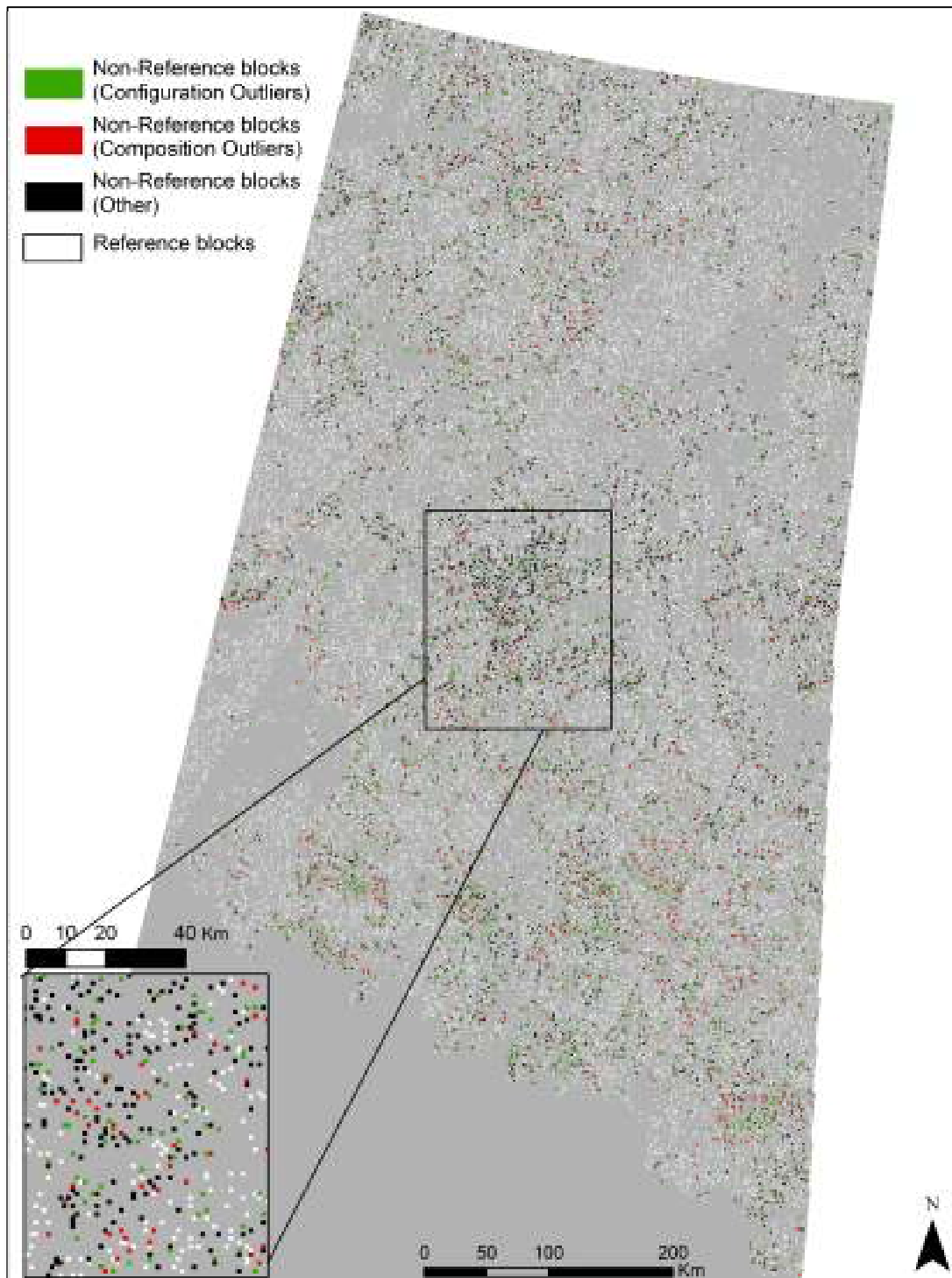


Figure 5. Nonreference sample blocks (1020 m × 1020 m) are those comprising a mixture of sensor types, image years, or image DOY. Blocks are highlighted where species composition and configuration values were outside the 5th–95th percentile of values.